STRUCTURAL AND ELECTRONIC PROPERTIES OF PENTACENE/PENTACENEQUINONE THIN FILMS PREPARED BY LANGMUIR–BLODGETT TECHNIQUE

Martin WEIS[a], Katarína GMUCOVÁ[b,*], Daniel HAŠKO[c] and Jarmila MÜLLEROVÁ[d]

[a] *Faculty of Electrical Engineering and Information Technology, Slovak University of Technology, Ilkovičova 3, SK-81219 Bratislava, Slovak Republic; e-mail: martin.weis@stuba.sk*

[b] *Institute of Physics, Slovak Academy of Sciences, Dúbravská cesta 9, SK-84511 Bratislava, Slovak Republic; e-mail: katarina.gmucova@savba.sk*

[c] *International Laser Center, Slovak University of Technology, Ilkovičova 3, SK-81219 Bratislava, Slovak Republic; e-mail: daniel.hasko@stuba.sk*

[d] *Department of Engineering Fundamentals, Faculty of Electrical Engineering, University of Žilina, ul. kpt. J. Nálepku 1390, SK-03101 Liptovský Mikuláš, Slovak Republic; e-mail: mullerova@lm.uniza.sk*

Received November 19, 2008
Accepted February 27, 2009
Published online March 25, 2009

Structural and electronic properties of pentacene/pentacenequinone thin films prepared on various solid-state substrates by the Langmuir–Blodgett technique are reported. Amorphous structure of the prepared films has been proved by XRD measurements. Oxygen-related defects have been identified in the Langmuir–Blodgett films as a consequence of the exposure of pentacene Langmuir layer to air. Crystallization induced by thermal treatment of the prepared amorphous thin films has been observed. Electronic properties of pentacene/pentacenequinone Langmuir–Blodgett films have been investigated in the contact-less architecture using electrochemical techniques. The energy band diagram of the amorphous pentacene/pentacenequinone Langmuir–Blodgett film on a metallic surface was constructed from the obtained electrochemical data.

Keywords: Pentacene; Monolayers; Thin films; Langmuir–Blodgett technique; Electrochemistry; X-ray diffraction; Atomic force microscopy.

In the last decade the electronic research has been focused on a variety of novel organic materials. Among them pentacene (PEN), a small molecular semiconductor with carrier mobility significantly higher than expected for standard polymer semiconductors, is of a great importance[1]. PEN as an active layer is a promising material for organic field effect transistors[2], organic light-emitting diodes and phototransistors[3], organic solar cells[4], and hydrogen storage films[5].

doi:10.1135/cccc2008210

Pentacene thin films on various substrates have been prepared by the standard techniques either from the solid phase[2a,6], or from solution[2a,7]. Solution-processed PEN thin films prepared by thermal conversion of 13,6-*N*-sulfinylacetamidopentacene have shown similar features as vacuum sublimated PEN [8]. Solving problems of the instability phenomena in the PEN-based devices is crucial for the future progress in organic and hybrid organic/inorganic electronics. The instability of PEN thin films has been studied from the viewpoints of molecular structural ordering and the interface state modification[9].

The energy bands of thin-film, bulk, and single-crystal phases of PEN were calculated[6d] and the relation between the crystal structure and energy dispersion was explained. Pentacenequinone (PQ) impurities have been introduced into a PEN material in a controlled manner to study the influence of their contents on thin film properties[10]. The impact of growth properties of a PEN thin film on the device performance was discussed[11]. The influence of top layer geometries on electronic properties of PEN thin films was studied[12]. Moreover, it has been shown that PEN thin film structures are strongly influenced by the type of the substrate used[13].

The growth phenomena in organic thin film preparation are due to orientational transitions and new scaling exponents fundamentally different from those observed in their inorganic counterparts. It is possible that the improvement of the understanding of various PEN thin film growth mechanisms will further promote the progress in organic and hybrid electronics. Several interesting challenges lie ahead for pentacene-based electronics. Among them, the growth of thin films on various surfaces has attracted significant attention. However, the crucial problems of molecular order control and thin film crystallinity have not been solved, yet.

The Langmuir–Blodgett (LB) method based on the layer-by-layer deposition of organic molecules is frequently used for the preparation of solution processed organic thin films as an alternative method to spin-coating, dip-coating or drop-casting. Primarily it was developed for the preparation of well-ordered monomolecular layers and multilayer films composed of amphiphilic organic molecules having hydrophilic head and hydrophobic tail. In the course of a LB film preparation an insoluble monolayer of a specific surface pressure-area state is formed at the air/water interface by a movable barrier. Subsequently, the monolayer is transferred onto a solid substrate. The variability of the obtained physical properties can be utilized for the material design and interlayer structure applications. This technique has been used for solution-processed films subsequently thermally converted to PEN [8]. Defect states formation in LB PEN films prepared without

any precursor has been reported and the results have been compared with the data obtained on evaporated films[14].

In the present study the application of the LB technique with a possibility of controlling intermolecular distance for PEN thin film deposition with the expected flat molecular orientation is described. Moreover, a detailed study of selected structural and electronic properties of the prepared films is performed.

EXPERIMENTAL

Materials and Sample Preparation

Pentacene (PEN; purchased from Sigma–Aldrich) was used for LB film deposition without further purification. The PEN solubility in the aromatic solvents such as *o*-dichlorobenzene[15] and 1,2,4-trichlorobenzene[16] has been recently reported. The Langmuir layer was formed on a water subphase stabilized at 17 °C using a PEN solution in a toluene–benzene mixture (1:1) heated to 80 °C. The film deposition was carried out at the surface pressure 10 mN/m with the dipping speed 5 mm/min.

Pentacene is soluble in organic solvents only at higher temperatures, however oxygen defects (pentacenequinone, PQ) from the ambient air provide the solubility also at the room temperature as PQ is a polar molecule. A PEN/PQ solution was spread on the subphase using a microsyringe. As a subphase the pure water (bidistilled and deionized, 15 MΩ cm) was used. The subphase was stabilized at 17 °C; the monolayer was allowed to equilibrate and the solvent to evaporate for 15 min, the surface pressure–area isotherm is shown in Fig. 1. Several surface-hydrophobic substrates (gold, platinum, Corning optical glass, and silicon wafer with SiO_2 layer hydrophobized by hexamethyldisilazane applied from the gas phase) were used for preparation of Langmuir–Blodgett (LB) films. The surface pressure 10 mN/m and the dipping speed 0.08 mm/s were used for the LB deposition of various films thicknesses. Sample annealing (thermal treatment) at 50, 100, 150 and 200 °C was performed in nitrogen atmosphere for 10 min.

All the chemicals used were of analytical grade, solution for electrochemical experiment (1 mM hydrochloric acid) was prepared in bidistilled water.

Experimental Techniques

Surface pressure–area isotherms of organic monomolecular layers on the air/water interface (Langmuir film) are widely used for the analysis of processes at the molecular level. In the present work, the surface pressure–area isotherms were measured by the Wilhelmy plate method with an accuracy of ±0.05 mN/m with surface pressure sensor PS4 (Nima Technology, UK). The isotherms strongly depend on various external conditions and material properties (pH, formation of domain structure, etc.). Hence, the monolayer analysis based merely on the obtained isotherms can lead to a misinterpretation[17] and the application of independent methods is necessary.

Dielectric properties of PEN films are often evaluated by the measurement of Maxwell's displacement currents[18]. This technique is based on the measurement of the deviation of the monolayer polarization due to the change in the induced electric charge. In our case,

the dynamic processes in the monolayer associated with the change in the charge distribution caused by its mechanical compression (the induced charge on the top electrode) varies with time, and a current flowing through the outer circuit via an electrometer is generated. The experimental setup attached to the computer-controlled model Langmuir trough (model 611, Nima Technology, UK) is as follows. The top electrode was aligned parallel to the interface (in air) without any direct (mechanical or electric) contact with a floating monolayer. The distance between the top electrode and the water surface was adjusted to a given air-gap (ca. 1 mm) by measuring the capacitance of the electrode system. The displacement current was detected with a Keithley 617 electrometer (Keithley Instruments, Cleveland, Ohio, USA). The total working area of the trough was 600 cm^2 and the compression rate was 50 cm^2/min, which corresponds to 0.17 $Å^2$/s per one molecule. The area of the top electrode was A_E = 20 cm^2. In contrast to the surface pressure–area isotherm, the analysis in Maxwell's displacement current measurement is extremely sensitive also in the low-surface-pressure area, where surface pressure methods are useless. A comparison of the surface pressure–area and the dipole moment projection–area isotherms is shown in Fig. 1.

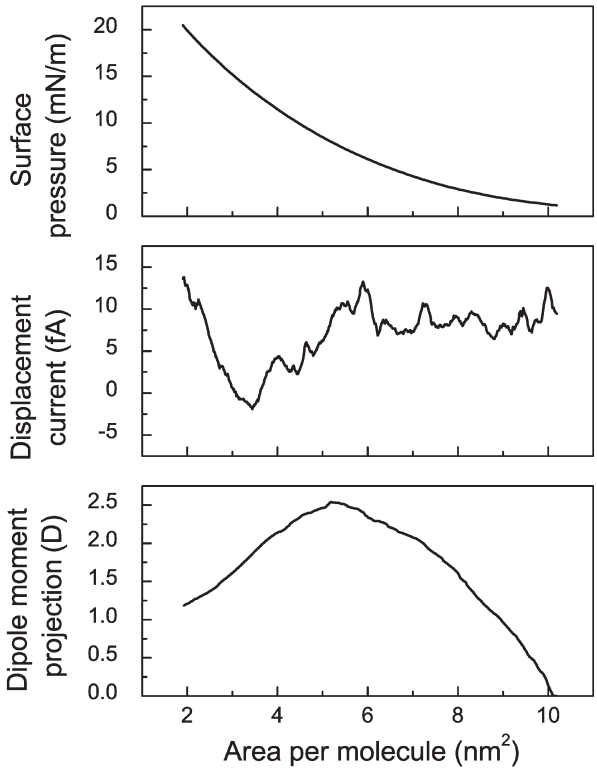

FIG. 1
Surface pressure–area (top), displacement current–area (middle), and dipole moment projection–area (bottom) isotherms of PEN/PQ monolayer

The data for X-ray diffraction (XRD) were collected on a Bruker D8 X-ray diffractometer by specular scans (Θ/2Θ) using CuK_α radiation (λ = 1.54 Å). The laser ellipsometry (SE400, λ = 632.8 nm, SENTECH, Germany) at the constant angle geometry (70°) was used for the monolayer thickness analysis as well as for quality monitoring of the deposition process. Surface topography, roughness analysis, and film thickness measurement (AFM nanometer profilometry) was performed by atomic force microscopy (AFM; high-resolution microscope Solver P47-PRO). To minimize the surface roughness in both the thickness and surface topology experiments, ten-monolayer stacks of PEN LB films were deposited on hydrophobized silicon wafer. Electrochemical experiments were performed in a three-electrode electrochemical cell equipped with an Ag|AgCl reference electrode and a Pt counter-electrode. The working electrode consisted of a round gold sheet (of 1.5 mm in diameter) covered with a 16 Langmuir–Blodgett layer stack of PEN. The scan rates of cyclic voltammetry and steady-state voltammetry were 100 and 3.33 mV/s, respectively.

Depending on the used experimental method a suitable thickness of the deposited thin film had to be chosen. Therefore, PEN LB films containing from 10 to 400 monolayers were studied in the present work. Seeing that we discuss properties of an organic semiconductor with the semiconductivity exhibited by its single molecules, we do not suppose a meaning effect of the film thickness on the electronic properties of this material.

RESULTS AND DISCUSSION

Langmuir Film Analysis

Mechanical properties of organic films are crucial for many applications; hence, their estimation before the layer deposition is essential. The elastic modulus (also called reciprocal compressibility) characterizes the rigidity of the monolayer and analogously to bulk materials is defined as

$$|E| = -A\left(\frac{\partial \pi}{\partial A}\right)_T \qquad (1)$$

where π stands for the surface pressure, A for the area per molecule and T for temperature. The elastic modulus of PEN Langmuir film (shown in Fig. 2) exhibits the maximal film strength for the areas per molecule corresponding with surface pressure of 10 mN/m, hence this value was chosen for the Langmuir–Blodgett films deposition.

In the used experimental setup the observed dynamic charge processes are caused by the lateral compression of the monolayer with the moveable barrier. Therefore, any time-independent charge (caused by a particularly structured water layer and some additional substances in the subphase) distributed near/at the interface has no effect. The major advantages of this method are the high sensitivity and explicitness of the measurement evalu-

ation. As was shown in previous studies[18,19], the current flowing in the outer circuit can be expressed as a time change of the induced charge

$$I = \frac{\partial Q_i}{\partial t} = \mu N \Gamma \frac{\partial \langle \cos \Theta \rangle}{\partial t} + \mu \langle \cos \Theta \rangle \Gamma \frac{\partial N}{\partial t} \qquad (2)$$

where μ is the dipole moment of molecule (μ_z is its projection to the normal), N is the number of molecules under the top electrode and Γ is the geometrical factor depending only on the distance between the top electrode and top plane of the monolayer, and on the shape and area of the upper electrode. The $\langle \cos \Theta \rangle$ stands for the statistical mean value of $\cos \Theta$, where Θ is the angle between the vector of dipole moment and the normal. By integrating the displacement current with respect to time, the induced charge Q_i can be obtained. In this way we have evaluated the vertical component of the molecular dipole moment. Thus, the dipole moment projection onto the normal μ_z should be calculated as

$$\mu_z = \mu \langle \cos \Theta \rangle = \frac{1}{\Gamma} \int \frac{I}{N} \mathrm{d}t \,. \qquad (3)$$

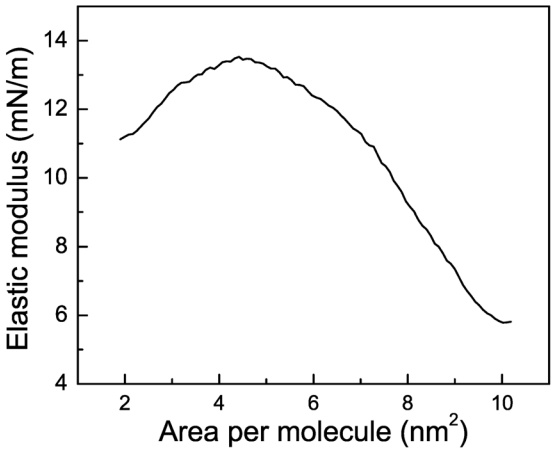

FIG. 2
Isothermal elastic modulus versus area per molecule

In this way the dipole moment projection, the molecular arrangement represented by $\langle \cos \Theta \rangle$, has been estimated (Fig. 1). The molecular dipole moment (maximal dipole moment projection) is 2.5 D.

To compare our measurement with theoretical predictions the molecular dipole moments were calculated by the parameterization method 3 (PM3)[20] for PEN, and for its oxygen-, hydrogen- and hydroxyl-related defects (Fig. 3). Quantum-mechanical computations were done using a MOPAC package[21]. Although all the above-mentioned defects generate a non-zero molecular dipole moment, only the creation of a single oxygen defect, i.e. 6-pentacenequinone, can be associated with our experimental results.

Langmuir–Blodgett Film Analysis

The specular XRD scan of the PEN/PQ LB film prepared on crystalline Si(200) is shown in Fig. 4. The structure of a polymer can be crystalline, partly crystalline, or amorphous. A fully or partly crystalline polymer gives sharp narrow diffraction peaks, while an amorphous polymer gives a broad peak. As is seen in Fig. 4, only an amorphous phase appears in the XRD for the PEN/PQ thin film prepared by the LB technique.

Optical properties of PEN/PQ layers recorded by laser ellipsometry are shown in Fig. 5. Since the recently measured optical properties of PEN/PQ

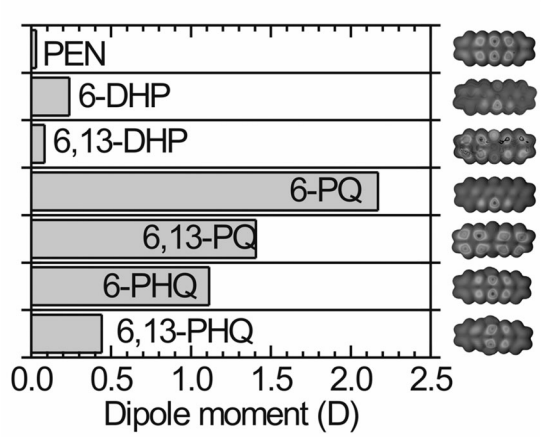

FIG. 3
Results of theoretical computations of the molecular dipole moments for pentacene (PEN) and its various defects: dihydropentacene (6-DHP, 6,13-DHP), pentacenequinone (6-PQ, 6,13-PQ) and pentacenehydroquione (6-PHQ, 6,13-PHQ). For each molecule, corresponding HOMO orbital is depicted

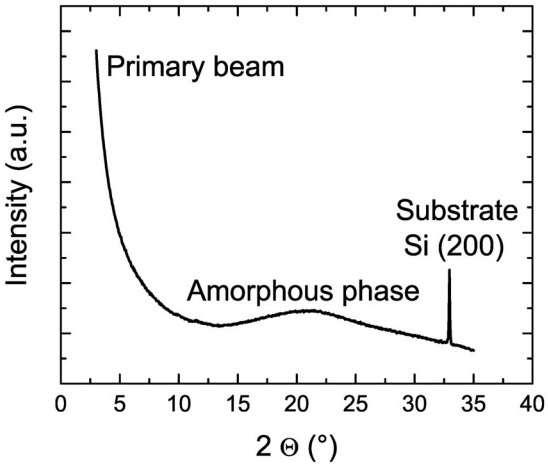

FIG. 4
XRD of the PEN/PQ LB film prepared on crystalline Si

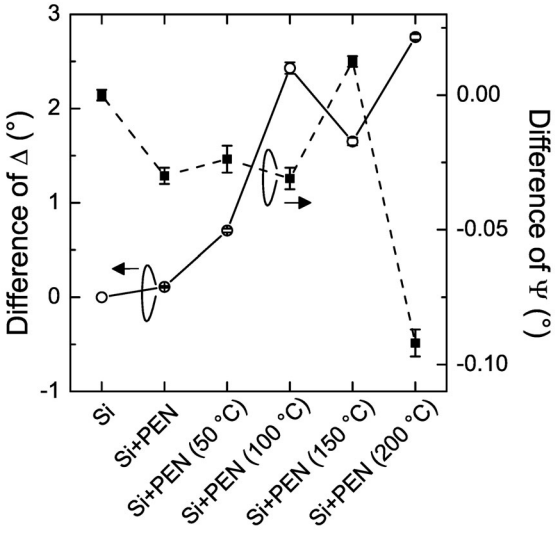

FIG. 5
Thermal evolution of ellipsometric parameters Ψ and Δ

have varied with the thickness and used deposition technique[22], only the directly measured optical parameters Ψ and Δ were analyzed as a deviation from the reference bare substrate to avoid the failure of the thickness simulation owing to a change of optical parameters by the annealing process. Deposition of the PEN/PQ layer is simply observable as a change of Δ parameter, which corresponds with the film thickness. Up to 150 °C, the film thickness seems to be constant, and then a rapid increase is observed. The Ψ parameter representing the contribution of absorbance changes only slightly, but its evolution is consistent with the dependence of Δ parameter. Hence, we can conclude that the film thickness and crystallization process will not rise below 150 °C. The surface topography for various temperatures is shown in Fig. 6. No surface structures after layer deposition have been observed as specific for the evaporated polycrystalline PEN [23]. Although after annealing the PEN/PQ LB film exhibits formation of granular structure, its surface still remains smooth without any significant increase in rough-

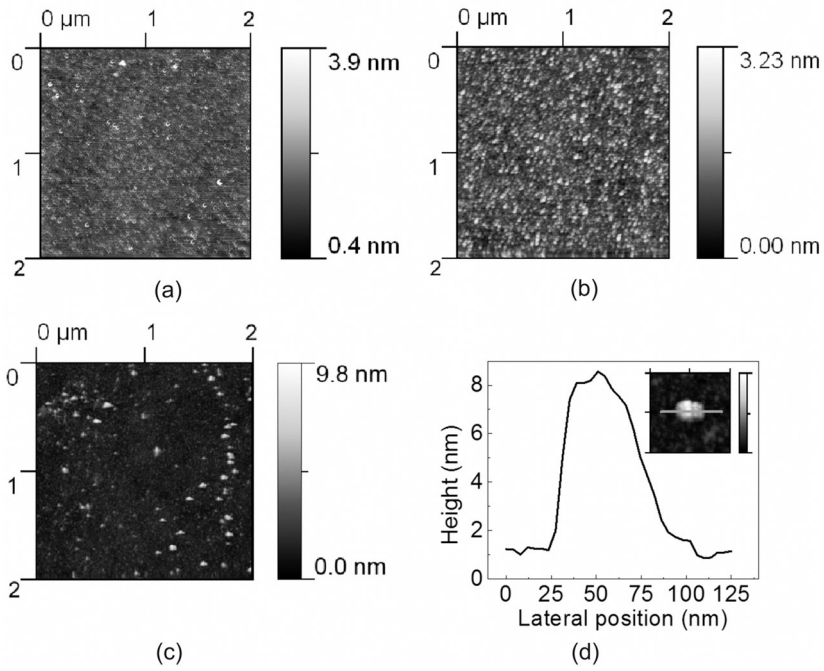

FIG. 6
Atomic force microscopy topography of PEN/PQ LB film: a as deposited, b annealed at 100 °C, c annealed at 200 °C, d cross-section of PEN nanocrystal shown in inset (image size 200 × 200 nm in plane, 8.5 nm full *z*-scale); detailed view taken from c

ness. For temperatures above 150 °C crystallization in some spike-like structures is achieved.

A summary of the topography and surface roughness is shown in Table I. AFM nanometer profilometry was used for the measurement of both the 200- and 400-layer thick LB PEN/PQ films, the thicknesses 100 and 200 nm being obtained, respectively. Hence, the monomolecular film thickness has been approximated to 0.5 nm.

TABLE I
Topography and surface roughness of the PEN/PQ LB film

PEN/PQ LB film	Topography max/average, nm	RMS roughness, nm
as deposited	4.9/1.1	0.2
at 50 °C	6.5/1.0	0.3
at 10 °C	9.1/1.3	0.4
at 150 °C	4.4/1.3	0.4
at 200 °C	9.8/1.8	0.6

Energy Band Diagram Construction

The knowledge of the band structure of semiconducting materials is essential for their further applications in microelectronics. Therefore, parameters such as ionization potential (IP), electroaffinity (EA), and energy gap (E_g) are important for understanding the properties of the prepared PEN LB films. The main point to be addressed now is to construct the energy band diagram of the amorphous PEN/PQ LB film from the experimental data obtained on the prepared samples.

Optical absorption of the PEN/PQ film with a thickness of 100 nm is depicted in Fig. 7. The obtained data have supported the presumption of the PQ presence in the LB film. The absorption spectrum exhibits peaks for the energies 2.94 and 3.12 eV, which is in accordance with the well-known values for PQ (2.94 and 3.11 eV)[24]. The energy gap E_g determines the threshold for the photon absorption in semiconductors; therefore the optical width of E_g can be evaluated from the absorption as an absorption edge (the intersection of the two slopes drawn at the maximum absorption and the background absorption in the electronic spectra, depicted in Fig. 7). We have obtained the E_g optical width of 2.55 eV.

Electrochemical measurements can provide information about electric properties of a thin organic film. Unlike the standard electric techniques the electrochemical measurements performed in aqueous environment are not influenced by the evaporated top-metal electrode. On the other hand, one must take into account possible formation of water-related defects in the PEN film during the experiment. The cyclic voltammogram depicted in Fig. 8 shows a quasireversible redox process. Here, both the oxidation and reduction are observed at +0.093 V (anodic scan) and at –0.156 V (cathodic scan), respectively. The ionization potential is directly related to the oxidation of the PEN/PQ molecules with respect to the reference electrode. It is necessary to correct these potentials using the vacuum level reference; for the standard hydrogen electrode (SHE) it is the energy 4.6 eV [25] on the assumed zero vacuum-level. Then the oxidation potential onset is E'_{ox} = 0.02 V, and the IP can be evaluated as

$$\mathrm{IP} = E'_{ox}\, e + 4.4\ \mathrm{eV} = 4.42\ \mathrm{eV} \qquad (4)$$

where the Ag|AgCl electrode potential was added to the SHE vacuum level reference potential (0.2 V). Afterwards, the electron affinity EA can be simply estimated[26] as EA = IP – E_g = 1.87 eV. This allows to determine the HOMO level in the energy diagram. We assume PQ molecule as a defect state of PEN, i.e., we are dealing with the well-known P-type organic semi-

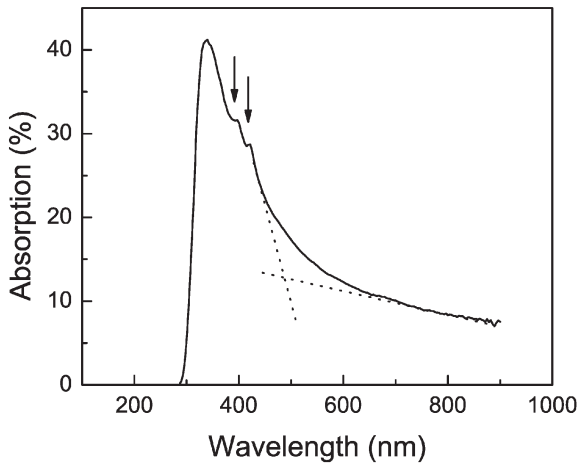

FIG. 7
Optical absorption of the PEN/PQ LB film deposited onto the Corning optical glass. The absorption spectrum exhibits peaks for energies 2.94 and 3.12 eV

conductor. Therefore, the steady state voltammetry in the negative potential must reflect the hole injection barrier on the metal/PEN interface. Steady-state voltammetry scans were performed for temperatures from 5 up

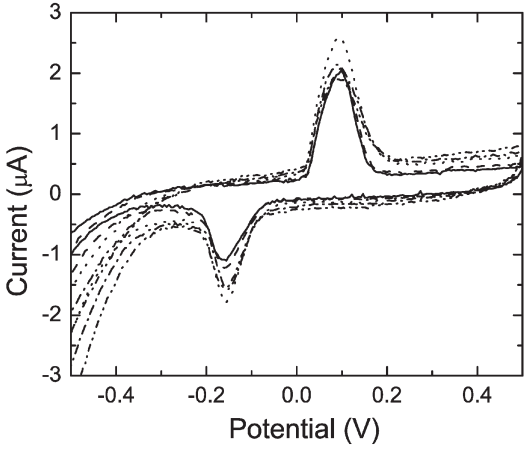

FIG. 8
Cyclic voltammograms of the PEN/PQ LB film at temperatures 10 (full line), 20 (dash line), 30 (dot line), 40 (dash-dot line) and 50 °C (dash-dot-dot line)

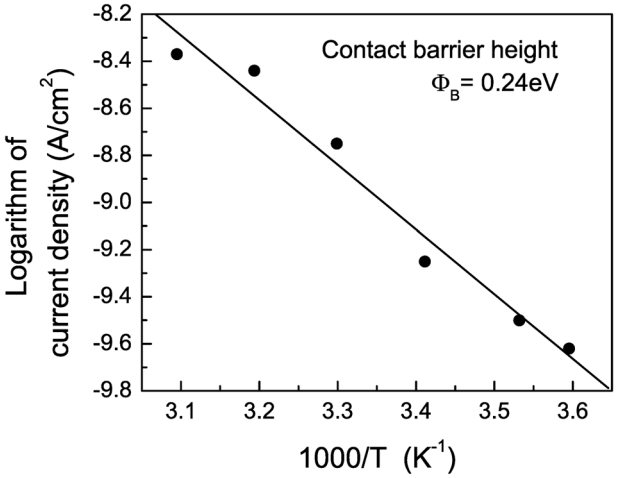

FIG. 9
Arrhenius plot of the current densities obtained from the steady state voltammetry scans at various temperatures (5, 10, 20, 30, 40 and 50 °C) at the potential –1 V

to 50 °C; the corresponding Arrhenius plot for the current densities at the potential –1 V is depicted in Fig. 9. The contact barrier height (i.e., the hole injection barrier) of the PEN/Au interface was estimated to be 0.23 eV. Finally, it is possible to construct the energy band diagram (without the bands bending on the interface) from this analysis (Fig. 10). Here, it is necessary to note that the estimated work function of a gold electrode (~4.7 eV) is in accordance with the experimental results obtained by the Kelvin probe surface potential measurement of a gold surface untreated with a ultraviolet lamp, i.e., 4.8 eV [27].

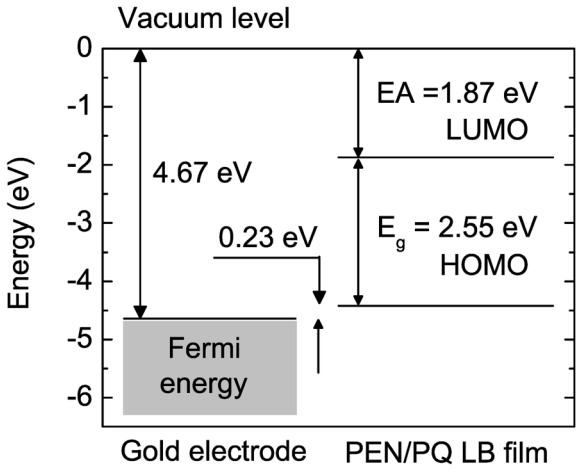

FIG. 10
Sketch of energy band diagram of PEN/PQ LB film deposited on the gold surface

CONCLUSIONS

Structural and electronic properties of Langmuir films and their relation to the PEN defects were studied. The observed value of molecular dipole moment corresponds to the formation of oxygen-related defect; this fact is in accordance with the absorption spectrum. Prepared layers exhibit an amorphous character proved by XRD analysis. The following thermal treatment in nitrogen atmosphere induced crystallization, a granular structure has been revealed. The crystallization process was probed by both the atomic force microscopy (AFM) and laser ellipsometry. Above 150 °C a spike-like PEN crystals were observed. Electronic properties of PEN/PQ LB films have been investigated using electrochemical techniques, too. The

energy band diagram of the amorphous PEN/PQ LB film prepared on metallic surface has been constructed.

The authors thank Dr. Ján Jakabovič for help with LB films annealing and Prof. Tibor Hianik for his help with laser ellipsometry. This research was supported by the Slovak Grant Agency VEGA (contracts No. 2/7118/27 and No. 1/3038/27) and the Slovak Research and Development Agency (contracts No. APVV-0267-06 and No. APVV-0290-06).

REFERENCES

1. a) Anthony J. E.: *Angew. Chem. Int. Ed.* **2008**, *47*, 452; b) Koch N.: *ChemPhysChem* **2008**, *8*, 1438; c) Halik M., Klauk H., Zschieschang U., Schmid G., Dehm C., Schütz M., Maisch S., Effenberger F., Brunnbauer M., Stellacci F.: *Nature* **2004**, *431*, 963; d) Stadlober B., Zirkl M., Beutl M., Leising G., Bauer-Gogonea S., Bauer S.: *Appl. Phys. Lett.* **2005**, *86*, 242902.
2. a) Dimitrakopulos C. D., Malenfant P. R. L.: *Adv. Mater.* **2002**, *14*, 99; b) Newman Ch. R., Frisbie C. D., da Silva Filho D. A., Brédas J.-L., Ewbank P. C., Mann K. R.: *Chem. Mater.* **2004**, *16*, 4436; c) Katz H. E.: *Chem. Mater.* **2004**, *16*, 4748; d) Madec M.-B., Crouch D., Llorente G. R., Whittle T. J., Geoghegan M., Yeates S. G.: *J. Mater. Chem.* **2008**, *18*, 3230; e) Benor A., Hoppe A., Wagner V., Knipp D.: *Org. Electron.* **2007**, *8*, 749.
3. a) Zhang F., Xu Z., Zhao S., Zhao D., Yuan G., Cheng Z.: *Appl. Surf. Sci.* **2008**, *255*, 1942; b) El Amrani A., Lucas B., Moliton A.: *Thin Solid Films* **2008**, *516*, 1626; c) Nakada H.: *J. Photopolym. Sci. Technol.* **2007**, *20*, 35; d) Ryu G. S., Choe K. B., Song C. K.: *Thin Solid Films* **2006**, *514*, 302.
4. a) Palilis L. C., Lane P. A., Kushto G. P., Purushothaman B., Anthony J. E., Kafafi Z. H.: *Org. Electron.* **2008**, *9*, 747; b) Sullivan P., Jones T. S.: *Org. Electron.* **2008**, *9*, 656; c) Yoo S., Domercq B., Kippelen B.: *Appl. Phys. Lett.* **2004**, *85*, 5427.
5. Fang B., Zhou H., Honma I.: *Appl. Phys. Lett.* **2006**, *89*, 023102.
6. a) Reynolds S., Shepherd J. T., Main C., Marshall J. M., Maud J. M.: *J. Non-Cryst. Solids* **2000**, *266–269*, 994; b) Schreiber F.: *Phys. Status Solidi A* **2004**, *201*, 1037; c) Shekar B. C., Lee J. Y., Rhee S. W.: *Korean J. Chem. Eng.* **2004**, *21*, 267; d) Hong S., Amassian A., Woll A. R., Bhargava S., Ferguson J. D., Malliaras G. G., Brock J. D., Engström J. R.: *Appl. Phys. Lett.* **2008**, *92*, 53304.
7. a) Shin S.-I., Kwon J.-H., Kang H., Ju B.-K.: *Semicond. Sci. Technol.* **2008**, *23*, 85009; b) Brown A. R., Pomp A., Hart C. M., de Leeuw D. M.: *Science* **1995**, *270*, 972; c) Brown A. R., Jarrett C. P., de Leeuw D. M., Matters M.: *Synth. Met.* **1997**, *88*, 37; d) Park J., Lee S., Lee H. H.: *Org. Electron.* **2006**, *7*, 256.
8. Musumeci Ch., Cascio C., Scandurra A., Indell G. F., Bongiorno C., Ravesi S., Pignataro B.: *Surf. Sci.* **2008**, *602*, 993.
9. Park C. B., Yokoyama T., Nishimura T., Kita K., Toriumi A.: *J. Electrochem. Soc.* **2008**, *155*, H575.
10. Conrad B. R., Gomar-Nadal E., Cullen W. G., Pimpinelli A., Einstein T. L., Williams E. D.: *Phys. Rev. B* **2008**, *77*, 5328.
11. Nickel B., Fiebig M., Schiefer S., Goellner M., Huth M., Erlen C., Lugli P.: *Phys. Status Solidi A* **2008**, *205*, 526.
12. Scharnberg M., Adelung R., Faupel F.: *Phys. Status Solidi A* **2008**, *205*, 5578.

13. a) Zheng Y., Qi D., Chandrasekhar N., Gao X., Troadec C., Wee A. T. S.: *Langmuir* **2007**, *23*, 8336; b) Chen Q., McDowall A. J., Richardson N. V.: *Langmuir* **2003**, *19*, 10164; c) Bavdek G., Cossaro A., Cvetko D., Africh C., Blasetti C., Esch F., Morgante A., Floreano L.: *Langmuir* **2008**, *24*, 767.
14. Nádaždy V., Durný R., Puigdollers J., Voz C., Cheylan S., Weis M.: *J. Non-Cryst. Solids* **2008**, *354*, 2888.
15. Tao C.-L., Zhang X.-H., Zhanga F.-J., Liub Y.-Y., Zhang H.-L.: *Mater. Sci. Eng. B* **2007**, *140*, 1.
16. Minakata T., Natsume Y.: *Synth. Met.* **2005**, *153*, 1.
17. Möhwald H. in: *Handbook of Biological Physics* (R. Lipowsky and E. Sackmann, Eds), Vol. 1, p. 164. Elsevier, Leiden 1995.
18. a) Iwamoto M., Majima Y.: *J. Chem. Phys.* **1991**, *94*, 5135; b) Iwamoto M., Wu C. X.: *Phys. Rev. E* **1996**, 54, 6603.
19. Vajda J., Weis M., Barančok D., Cirák J., Tomčík P.: *Appl. Surf. Sci.* **2004**, *229*, 183.
20. Stewart J. J. P.: *J. Comput. Chem.* **1989**, *10*, 221.
21. Stewart J. J. P.: *Quantum Chem. Prog. Exch.* **1990**, *10*, 86.
22. a) Park S. P., Kim S. S., Kim J. H., Whang C. N., Im S.: *Appl. Phys. Lett.* **2002**, *80*, 2872; b) Hinderhofer A., Heinemeyer U., Gerlach A., Kowarik S., Jacobs R. M. J., Sakamoto Y., Suzuki T., Schreiber F.: *J. Chem. Phys.* **2007**, *127*, 194705.
23. Ruiz R., Mayer A. C., Malliaras G. G., Nickel B., Scoles G., Kazimirov A.: *Appl. Phys. Lett.* **2004**, *85*, 4926.
24. a) Hwang D. K., Kim K., Kim J. H., Jung D. Y., Kim E., Im S.: *Appl. Surf. Sci.* **2005**, *244*, 615; b) Itoh T.: *Chem. Rev.* **1995**, *95*, 2351.
25. a) Trasatti S.: *J. Electroanal. Chem.* **1983**, *150*, 1; b) Xie Q., Kuwabata S., Yoneyama H.: *J. Electroanal. Chem.* **1997**, *420*, 219; c) Bredas J. L. in: *Handbook of Conducting Polymers* (T. A. Skotheim, Ed.), Vol. 2, p. 859. Dekker, New York 1986; d) D'Andrade B. W., Datta S., Forresta S. R., Djurovich P., Polikarpov E., Thompson M. E.: *Org. Electron.* **2005**, *6*, 11.
26. Stockert D., Kessel R., Schultze J. W.: *Synth. Met.* **1991**, *41*, 1295.
27. Suzue Y., Manaka T., Iwamoto M.: *Jpn. J. Appl. Phys.* **2005**, *44*, 561.